A Reduced-Order Adaptive Velocity Observer for Manipulator Control

M. Erlic and W.-S. Lu

Abstract—**In this paper a new manipulator joint velocity observer is presented. The observer is reduced in its order and it is adaptive with respect to unknown dynamic parameters. The velocity estimate produced by the observer is used in an adaptive controller for trajectory tracking. The result is locally asymptotically stable velocity observation errors and locally asymptotically stable position and velocity trajectory tracking errors. Simulations of the proposed scheme on the PUMA-560 show an improvement over a well known adaptive controller which obtains its joint velocity estimates via numerical differentiation. Experiments demonstrate the usefulness of the proposed observer.**

I. Introduction

In this paper a new joint velocity observer for manipulators with unknown dynamic parameters is presented. This proposed observer calculates a smooth velocity estimate which is used by an adaptive controller for trajectory tracking. The adaptive observer presented here improves on other adaptive observers in two ways. First, the proposed observer does not use variable structure and switching to maintain stability. As a result chattering is largely eliminated. Second, the proposed observer is reduced in its order. This leads to a differential equation which has first order dynamics. Previous manipulator velocity observers have employed full order observers which have second order dynamics rendering a larger delay.

The computed torque (CT) controller [2] for manipulator trajectory control compensates exactly for the nonlinear dynamics of a robot manipulator and introduces a specified second order linear dynamics. But its performance depends on a precise knowledge of the dynamics parameters and accurate position and velocity measurements which may not be available always. Usually, a precise knowledge of the dynamic parameters for both the manipulator and its load is not completely available. Even for the popular manipulator such as the PUMA-560, for which the dynamic parameters have been accurately determined [1], performance degradation can be expected for variable payloads.

In order to overcome the limitations of the CT controller in the presence of unknown dynamic parameters and changing loads, controllers using adaptive mechanisms have been proposed [3], [6], [10]. In these, Lyapunov analysis and the special properties of the manipulator dynamics are adopted to design controllers which identify the manipulator's link or load parameters. The adaptive controllers proposed in [3], [6], [10] require low noise in the velocity measurements. In some circumstances velocity sensors may not be available and even when they are available, noise may be a problem as is the case with tachometers. Sensor noise places limits on controller gains, resulting in larger tracking errors. Velocity filtering is an option; however, a time delay is introduced which can not be accepted in high performance tracking. Alternatively, joint velocities can be determined by differentiating position measurements obtained with potentiometers or optical encoders. Usually, an optical encoder has a large signal to noise ratio; with differentiation, however, even low levels of noise in the position signal may produce unacceptably large velocity noise.

In order to eliminate the need for tachometers and numerical differentiation but maintain high control accuracy, one option is to use a joint velocity observer. Observers for linear systems were proposed by Luenberger [7]. The concept of the observer was tailored to estimate manipulator joint velocities in [8] and [12] where state-space approaches were used that yield observers with second order dynamics. In [5] a reduced-order manipulator velocity observer was proposed which has first order dynamics. In these papers observers have been proposed which assume an exact knowledge of the manipulator's dynamic parameters. In order to accommodate for cases where dynamic parameters are only partly known or are not known at all, an adaptive mechanism is required. In [13] an adaptive observer-controller was presented that uses variable structure compensation. Even though most of the high frequency switching is restricted to the numerical implementation of the observer, the switching might still excite unmodeled higher frequency dynamics.

In this paper a reduced-order adaptive observer is proposed where the joint position vector is considered a known "parameter" of the observer. The result is a reduction in the order of the observer. By avoiding the use of variable structure compensation, the signal produced by the observer is smooth and the excitation of higher frequency unmodeled dynamics is less likely. The new adaptive observer-controller has been applied to a PUMA-560 manipulator and the experimental results demonstrate that accurate tracking results can be achieved for industrial manipulators which provide the computer controller with position information only.

The paper is organized as follows. In Section II, the manipulator dynamic model is described and several useful properties are reviewed. Section III introduces the proposed adaptive observer and addresses the stability and implementation of the observer. Section IV presents the combined adaptive observer-controller and the stability of both the observation and tracking errors is shown. Simulation and experimental results are then presented in Section V.

II. Notation and Preliminaries

The dynamic equation of an n degree-of-freedom robot manipulator is given by

$$H(q)\ddot{q} + C(q,\dot{q})\dot{q} + F\dot{q} + g(q) = Y(q,\dot{q},\ddot{q})a = \tau \tag{1}$$

where $q \in \mathcal{R}^n$ is the joint position vector, $\tau \in \mathcal{R}^n$ is the vector of joint torques, $g(q) \in \mathcal{R}^n$ represents the gravitational torques, $H(q) = I_r(q) + I_m \in \mathcal{R}^{n\times n}$ is a matrix consisting of the rigid link inertia matrix $I_r(q)$ and motor and gear inertia matrix I_m. $C(q,\dot{q})\dot{q} \in \mathcal{R}^n$ is the vector of Coriolis and centripetal torques, $F = K_\omega + V \in \mathcal{R}^{n\times n}$ is a diagonal matrix consisting of the back emf coefficient matrix K_ω and the viscous friction coefficient matrix V. $Y(q,\dot{q},\ddot{q}) \in \mathcal{R}^{n\times p}$ is a regressor matrix and $a \in \mathcal{R}^p$ is a vector of dynamic parameters.

In this paper it is assumed that the joint position measurements q are available but that joint velocities $\dot{q}$ are not. Several properties of the manipulator dynamic equation useful in the subsequent development are summarized as follows:

Manuscript received December 15, 1992; revised March 14, 1994. This work was supported by the Science Council of British Columbia and IRIS Network of Centres of Excellence Program of Canada in Robotics and Intelligent Systems.

The authors are with the Department of Electrical and Computer Engineering, University of Victoria, Victoria, British Columbia, Canada V8W 3P6.

IEEE Log Number 9408211.

1042-296X/95$04.00

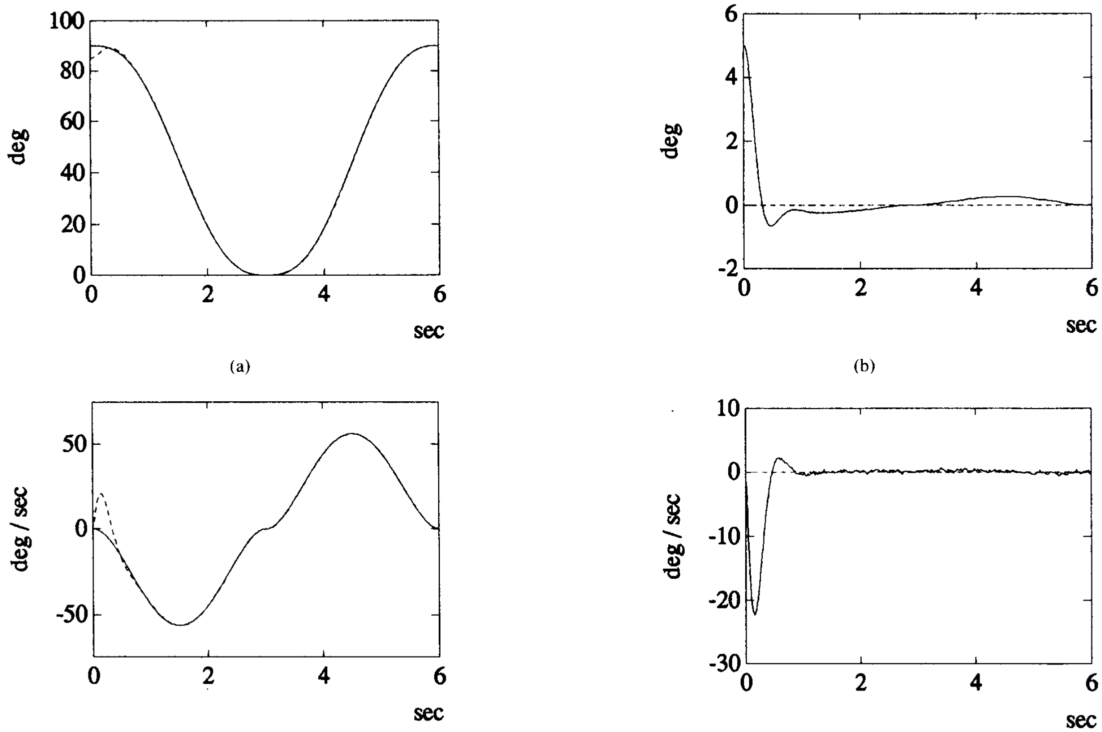

Fig. 1. Simulation results for the first link using the adaptive observer (a) desired versus actual position, (b) position error, (c) desired versus actual velocity, (d) velocity error.

Property 1: The manipulator inertia matrix is positive definite, symmetric and bounded, i.e. $m_l \le \|H(q)\| \le m_u$ where $m_l, m_u > 0, \forall q \in \mathcal{R}^n$.

Property 2: The 2-norm of $C(q,x)$ is bounded, i.e.

$$\|C(q,x)\| \le m_c\|x\|, \qquad m_c > 0, \forall q, x \in \mathcal{R}^n. \tag{2}$$

Property 3: The matrix of Christoffel symbols, $C(q,x)$ satisfies $C(q,x)\xi = C(q,\xi)x \ \forall q, x, \xi \in \mathcal{R}^n$ where the matrix of Christoffel symbols is uniquely defined in [11].

Property 4: $\dot{H}(q) - 2C(q,\dot{q})$ is skew symmetric.

Property 5: The manipulator dynamic equation is linear in its parameters of interest, i.e.

$$H(q)\upsilon + C(q,\xi)\xi + F\xi + g(q) = Y(q,\xi,\Psi)a \tag{3a}$$

$$H(q)\upsilon + C(q,x)\xi + F\xi + g(q) = Y(q,\xi,x,\upsilon)a \tag{3b}$$

$\forall q, \xi, x, \upsilon \in \mathcal{R}^n$ and $\forall a \in \mathcal{R}^p$ where p is the number of dynamic parameters. Matrix Y in (3) is usually known as the manipulator regressor [10].

III. The Adaptive Velocity Observer

A. The Adaptive Observer

The manipulator dynamic (1) can be written as

$$\dot{x} = H^{-1}(q)[\tau - C(q,x)x - Fx - g(q)] \tag{4}$$

where $x = \dot{q}$. This expression can be considered a first order equation in x where q is assumed known. The principal part of the proposed observer has a structure similar to (4) and is given by

$$\dot{\hat{x}} = \upsilon(q,\hat{x},\tau,\hat{a}) + K\tilde{x} \tag{5a}$$

$$\upsilon(q,\hat{x},\tau,\hat{a}) = \hat{H}^{-1}(q)[\tau - \hat{C}(q,\hat{x})\hat{x} - \hat{F}\hat{x} - \hat{g}(q)] \tag{5b}$$

where $\hat{x}$ is the *observed* velocity estimate, $\tilde{x} = x - \hat{x}$ is the observation error, $K > 0$ is a diagonal gain matrix, and $(\hat{*})$ denotes the term $(*)$ with unknown parameters replaced by their estimates. Now let $a \in \mathcal{R}^p$ be the vector that collects the unknown parameters in the manipulator dynamics. The estimated parameters used in (5) are obtained with the following adaptation law

$$\dot{\hat{a}} = -\Gamma Y^T(q,\hat{x},\upsilon)\tilde{x} \tag{6}$$

where $Y(q,\hat{x},\upsilon)$ is the regressor determined by (3) and $\Gamma > 0$ is a diagonal gain matrix. If the manipulator starts from rest, one can take $\hat{x}(t_0) = 0$ where t_0 denotes the moment when the robot motion begins. Otherwise one has to make a guess for $x(t_0)$ and denote it by $\hat{x}(t_0)$. Similarly, one has to make a guess for the unknown parameter vector $\hat{a}(t_0)$ at $t = t_0$. Although it is very likely that these initial estimates are not accurate, it will be shown in Section III-C that the observer being developed here is locally asymptotically stable as long as the initial estimate errors are inside a region of attraction. Integrating (5a) and (6) over the time interval $[t_0, t]$ and using the estimated initial conditions $\hat{x}(t_0)$ and $\hat{a}(t_0)$, we obtain

$$\hat{x}(t) = y(t) + \int_{t_0}^{t} [\upsilon(q,\hat{x},\tau,\hat{a}) - K\hat{x}]\,dt \tag{7a}$$

where

$$y(t) = \hat{x}(t_0) + K[q(t) - q(t_0)] \tag{7b}$$

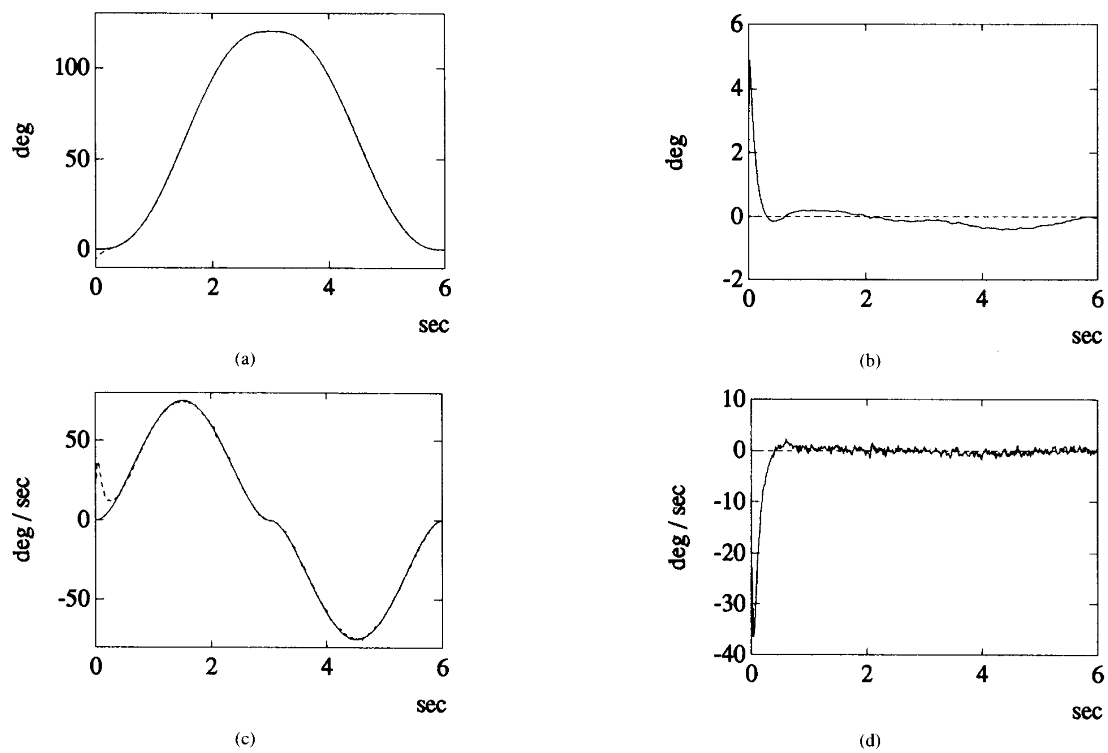

Fig. 2. Simulation results for the second link using the adaptive observer (a) desired versus actual position, (b) position error, (c) desired versus actual velocity, (d) velocity error.

is known, and

$$\hat{a}(t) = \hat{a}(t_0) - \Gamma \int_{t_0}^{t} Y^T(q, \hat{x}, v)\tilde{x}\, dt. \tag{8}$$

Using $\tilde{x} = x - \hat{x}$ with $x = dq/dt$, (8) becomes

$$\hat{a}(t) = \hat{a}(t_0) - \Gamma \int_{q(t_0)}^{q(t)} Y^T(q, \hat{x}, v)dq + \Gamma \int_{t_0}^{t} Y^T(q, \hat{x}, v)\hat{x}\, dt \tag{9}$$

where the first integral is carried out with respect to joint position q. The system of integral (7a) and (9), which are equivalent to (5) and (6) together with initial conditions $\hat{x}(t_0)$ and $\hat{a}(t_0)$, provides an equivalent version of the adaptive observer (5). The signal $\hat{x}(t)$, which is a part of the solution to this system of integral equations, is called the output of the observer.

It is important to stress that the observer (5), (6) is *not* implementable in case the velocity measurements are not available. This is because both (5a) and (6) involve the use of $\tilde{x} = x - \hat{x}$. Likewise, the observer characterized equivalently by (7) and (9) is also *not* implementable since the evaluation of $\hat{a}(t)$ using (9) (and therefore the evaluation of $\hat{x}(t)$ using (7a)) involves the differentiation of the joint position $q(t)$. As will be seen in the next subsection, however, an implementable approximation of the proposed observer does exist.

B. An Implementable Approximation of the Observer

From (7) and (9), it follows that for an arbitrary fixed time interval $\Delta < 0$,

$$\hat{x}(t) = \hat{x}(t - \Delta) + K[q(t) - q(t - \Delta)] + \int_{t-\Delta}^{t} [v(q, \hat{x}, \tau, \hat{a}) - K\hat{x}]\, dt \tag{10}$$

and

$$\hat{a}(t) = \hat{a}(t - \Delta) - \Gamma \int_{q(t-\Delta)}^{q(t)} Y^T(q, \hat{x}, v)dq + \Gamma \int_{t-\Delta}^{t} Y^T(q, \hat{x}, v)\hat{x}\, dt. \tag{11}$$

Assuming that $Y(q, \hat{x}, v)$, $v(q, \hat{x}, \tau, \hat{a})$ and the joint position $q(t)$ as time functions are continuous and that Δ is sufficiently small, (10) and (11) suggest a discrete implementation of the proposed observer as follows

$$\hat{x}(i) = (I - \Delta K)\hat{x}(i-1) + \Delta v(i-1) + K[q(i) - q(i-1)] \tag{12}$$

$$\hat{a}(i) = \hat{a}(i-1) + \Gamma Y^T(i-1)[\Delta \hat{x}(i-1) - q(i) + q(i-1)]. \tag{13}$$

Remarks:

1) Obviously, (12) and (13) represent only an approximation of the observer proposed in (7) and (9). They are however implementable, and they approach to (10) and (11) (and therefore (7) and (9)) as Δ approaches to zero. In other words, (12) and (13) stand for a good representative of the observer if the sampling interval Δ is sufficiently small.
2) A problem with the continuity of v in (12) and (13) could develop if the adaptation of $\hat{a}$ causes an ill conditioned $\hat{H}$. To remedy this, an adjustment given in [3] can be used to guarantee $\hat{H} > 0$.

C. Stability of the Observer

If the proposed adaptive observer is not used in control, the local asymptotic stability of the observation error is assumed by Theorem

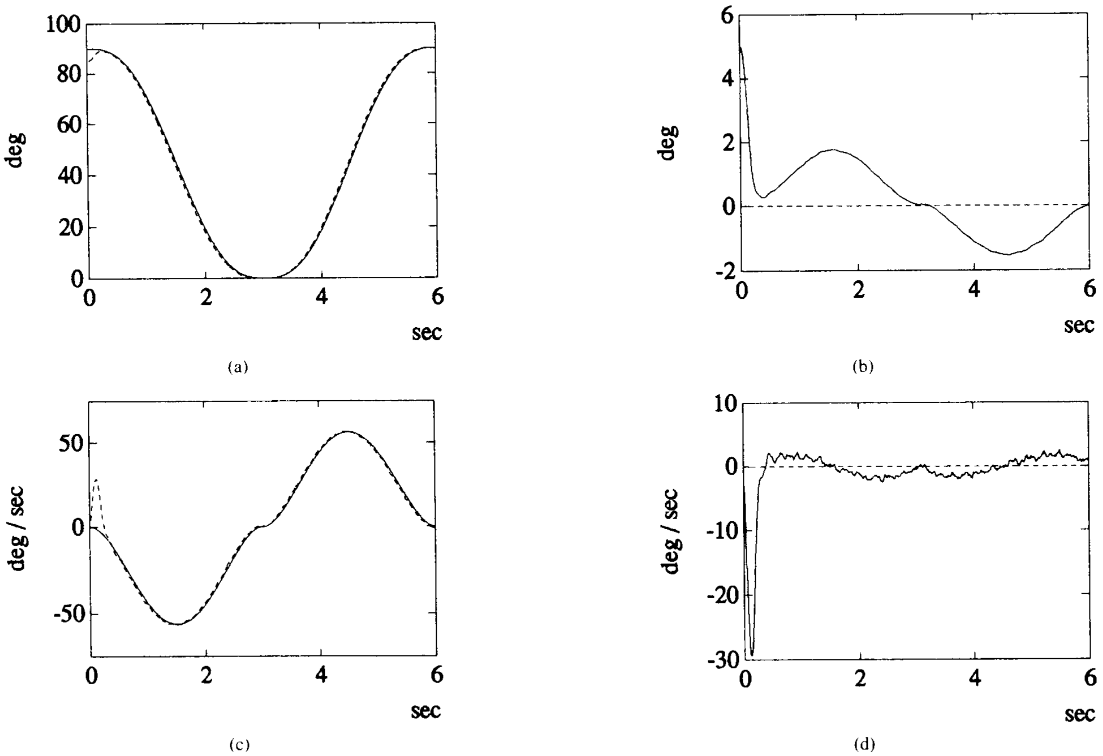

Fig. 3. Simulation results for the first link using Slotine-Li method with differentiation (a) desired versus actual position, (b) position error, (c) desired versus actual velocity, (d) velocity error.

1 which is stated below. For the sake of simplicity, in the rest of the paper we have taken $t_0 = 0$.

Theorem 1: For a given $K > 0$, $\tilde{x}(t) \to 0$ as $t \to \infty$ if $\|\tau(t)\|$ is bounded, $\|x(t)\| \leq m_v$,

$$\underline{\sigma} > m_c m_v + \beta - m_f \tag{14}$$

where $\underline{\sigma} = \lambda_{\min}(KH(q) + H(q)K)/2, \beta > 0$ is a fixed constant, $m_f = \lambda_{\min}(F)$, m_c is given in (2), and the initial estimation error $e(0) = [\tilde{x}^T(0)\,\tilde{a}^T(0)]^T$ belongs to the ball B_e defined by

$$B_e = \left\{ e(0) \in \mathcal{R}^{n+p} : \|e(0)\| < \sqrt{\frac{p_l}{p_u}}\left(\frac{1}{m_c}(\underline{\sigma} + m_f - \beta) - m_v\right)\right\}$$

where $p_l = \lambda_{\min}(P)$ and $p_u = \lambda_{\max}(P)$ with $P = \mathrm{diag}\{H(q), \Gamma^{-1}\}$.

A proof of Theorem 1 is given in Appendix A. The main assumptions made in Theorem 1 are that joint velocities and joint torques are bounded and the bound of $x(t)$ is known. Although these assumptions appear to be quite restrictive, the result of Theorem 1 can be interpreted as a quantitative relation of the region of attraction to the magnitude of joint velocity (among other things). In some circumstances the robot is controlled to move along a given trajectory so a reasonable upper bound of $\|x\|$ may be obtained by adding a sufficient tolerance to the desired joint velocity trajectory $\|\dot{q}_d\|$. More importantly, these assumptions will be eliminated when the proposed observer is combined with an adaptive controller in a feedback loop for robot motion control. Finally, Theorem 1 also quantifies the relation of observer gain K to the region of attraction, indicating how a gain matrix K is selected to make the observer work for a given $e(0)$. Furthermore, the region of attraction B_e is established as nontrivial since $\underline{\sigma}$ can be made as large as required to establish the inequality (14) for a fixed $\beta > 0$.

IV. Control with an Adaptive Velocity Observer

In this section the adaptive observer presented above is combined with an adaptive controller to realize a manipulator-observer-controller system which exhibits locally asymptotically stable trajectory tracking errors and locally asymptotically stable velocity observation errors.

A. The Controller

The proposed trajectory tracking controller is a variation of the controller proposed in [10] where the measured joint velocities are replaced by velocity estimates obtained with the proposed adaptive observer (5). The adaptive controller considered here is defined by

$$\begin{aligned}\tau = {} & \hat{H}(q)[\dot{x}_d - (\hat{x}_o - x_d)] + \hat{C}(q, \hat{x}_o)x_r \\ & + \hat{F}x_r + \hat{g}(q) - K_d\hat{s} - K_p\tilde{q}\end{aligned} \tag{15}$$

where $\hat{s} = \hat{x} - x_r$; the reference velocity is given by $x_r = x_d - \tilde{q}$ where $x_d(t)$ is the desired velocity trajectory; and the position tracking error is given by $\tilde{q} = q - q_d$ where $q_d(t)$ is the desired joint displacement trajectory. The proportional and derivative gain matrices are $K_p > 0$ and $K_d > 0$, respectively.

The adaptation rule employed to update the estimated dynamic parameters is given by

$$\dot{\hat{a}} = -\Gamma[Y^T(q, \hat{x}, x_r, \dot{x}_d)s + Y'^T(q, \hat{x}, v)\tilde{x}] \tag{16}$$

where $s = \tilde{q} + \dot{\tilde{q}}$ contains an unknown quantity x. Integrating (16) over $[0, t]$, we obtain an equivalent version of (16) where x

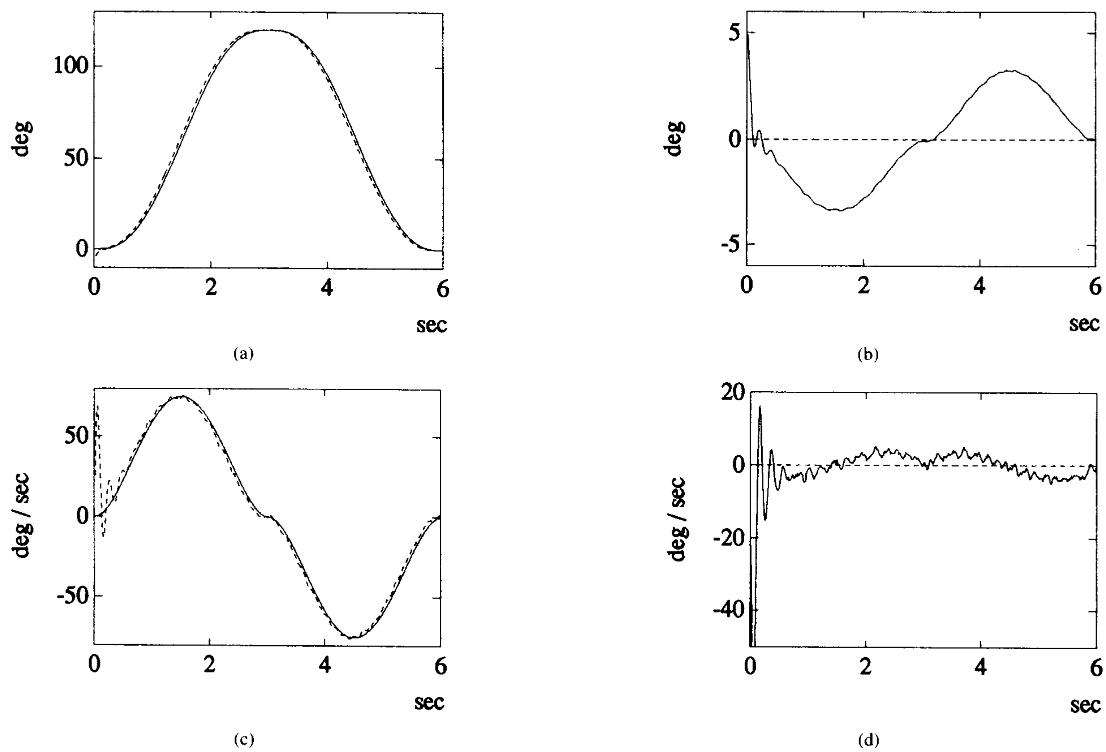

Fig. 4. Simulation results for the second link using Slotine-Li method with differentiation (a) desired versus actual position, (b) position error, (c) desired versus actual velocity, (d) velocity error.

is eliminated.

$$\hat{a}(t) = \hat{a}(t_0) - \Gamma \int_{q(0)}^{q(t)} (Y_{\rm obs} + Y_{\rm ctr})^t \, dq - \Gamma \int_0^t [\dot{Y}_{\rm obs}^T \hat{x} + \dot{Y}_{\rm ctr}^T (\tilde{q} - x_d)] \, dt \tag{17}$$

where $Y_{\rm obs} = Y(q, \hat{x}, v)$ and $Y_{\rm ctr} = Y(q, \hat{x}, x_r, \dot{x}_d)$. The estimated parameters obtained from (17) are used both in the observer (5) and the controller (15).

An approximate implementation of controller (15) involves simply the calculation of $\tau(t)$ at time instant $t = i\Delta$. For the implementation of the parameter estimator, it follows from (17) that

$$\hat{a}(t) = \hat{a}(t - \Delta) - \Gamma \int_{q(t-\Delta)}^{q(t)} (Y_{\rm obs} + Y_{\rm ctr})^T \, dq - \Gamma \int_{t-\Delta}^{t} [\dot{Y}_{\rm obs}^T \hat{x} + \dot{Y}_{\rm ctr}^T (\tilde{q} - x_d)] \, dt$$

which suggests an approximate implementation of (17) as follows

$$\begin{aligned} \hat{a}(i) = \hat{a}(i-1) &- \Gamma [Y_{\rm obs}(i-1) + Y_{\rm ctr}(i-1)]^T [q(i) \\ &- q(i-1)] - \Delta T [\dot{Y}_{\rm obs}^T (i-1) \hat{x}(i-1) \\ &+ \dot{Y}_{\rm ctr}(i-1)(q(i-1) - q_d(i-1) \\ &- x_d(i-1))] \end{aligned} \tag{18}$$

B. Stability of the Adaptive Observer-Controller

When the proposed adaptive observer is employed to provide a velocity signal which is used by the trajectory tracking controller given in (15), it can be shown that the position and velocity tracking errors as well as the observer velocity errors exhibit local asymptotic stability. This is established in Theorem 2 whose proof can be found in Appendix B.

Theorem 2: For given $K > 0$, $K_p = K_p^T > 0$, $K_d = k_d I > 0$ and $\Gamma > 0$, $\hat{x}(t), \tilde{q}(t), \dot{\tilde{q}}(t) \to 0$ as $t \to \infty$ if

$$\underline{\sigma} > c - \frac{b^2}{4a} - m_f + \beta \tag{19a}$$

and the initial estimate error $e(0)^T = [s^T(0)\, \tilde{x}_o^T(0)\, \tilde{q}^T(0)\, \tilde{a}^T(0)]$ belongs to the ball B defined by

$$B = \left\{ e(0) \in \mathcal{R}^{3n+p} : \|e(0)\| < \sqrt{\frac{p_l}{p_u}} \left[\frac{\sqrt{4a(\underline{\sigma} + m_f - \beta) + b^2 - 4ac} - b}{2a} \right] \right\}$$

where $\beta > 0$ is an arbitrary constant, $p_l = \lambda_{\min}(P), p_u = \lambda_{\max}(P)$ with $P = \mathrm{diag}(H(q), H(q), K_p, \Gamma^{-1}), \underline{\sigma} = \lambda_{\min}(KH(q) + H(q)K)/2$ and

$$a = \frac{m_c^2}{(k_d + m_f)} \tag{19b}$$

$$b = \left\{ \frac{1}{(k_d + m_f)} [2m_c^2 + m_d + 2m_c(k_d + m_u)] + 2m_c \right\} \tag{19c}$$

$$c = \frac{1}{(k_d + m_f)} \left\{ \frac{1}{4}(k_d + m_u)^2 + m_c^2 m_d^2 + 2m_c m_d (k_d + m_u) \right\} + m_c m_d \tag{19d}$$

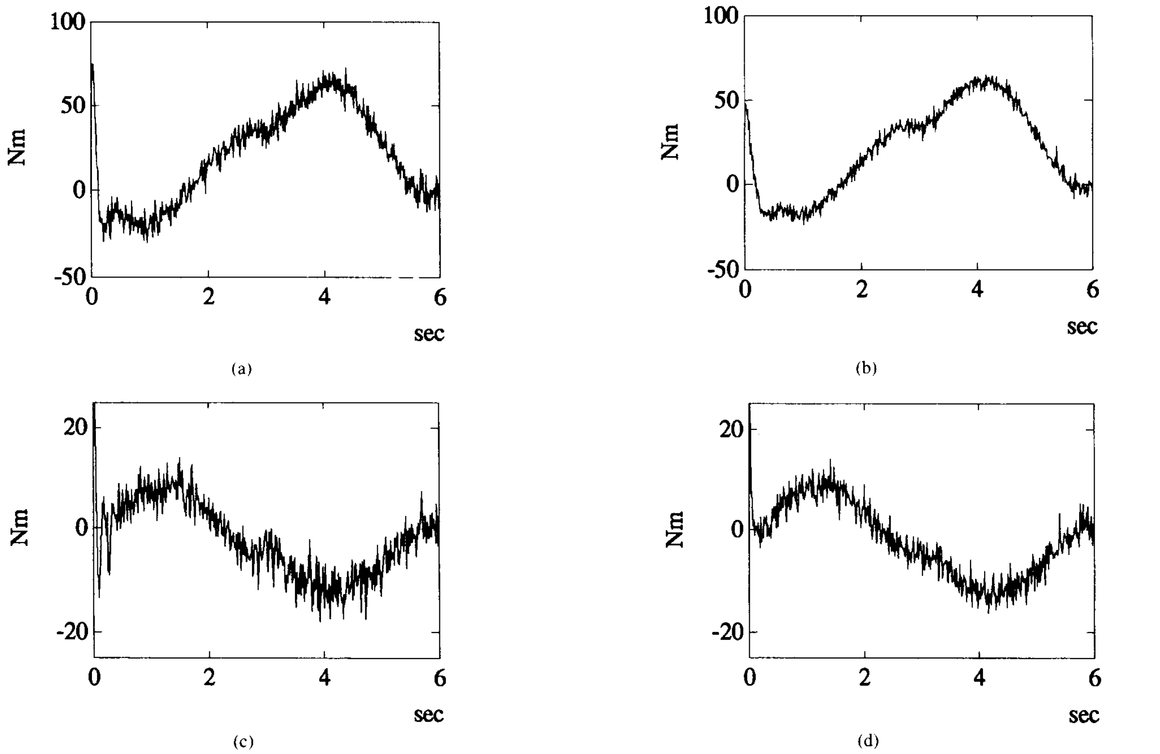

Fig. 5. Simulation: comparison of joint torques (a) Slotine-Li method with differentiation, joint 1, (b) adaptive observer method, joint 1, (c) Slotine-Li method with differentiation, joint 2, (d) adaptive observer method, joint 2.

V. Simulation and Experimental Results

In this section the performance of the proposed observer-controller will be demonstrated with simulations and experiments. The proposed system is compared with the well known Slotine-Li adaptive controller [10]. The proposed method uses an observer to obtain a velocity estimate, whereas the Slotine-Li method uses numerical differentiation. It will be shown that the proposed method has superior performance when the position measurement is corrupted with noise.

A. The Model

The second and third links of the PUMA-560 were used to demonstrate the performance of the proposed observer-controller in the presence of position measurement noise. In order to approximate continuous control more accurately PUMAs Mark II controller was modified [4], making a sampling frequency of 250 Hz possible. In this section, the second PUMA-560 link angle is considered joint angle one and the third link angle is considered joint angle two. The fourth, fifth and sixth links of the PUMA-560 were fixed. As such they constituted the third link of the robot; the mass of this last link was denoted by m_3. In the experiment it was assumed that m_3 was an unknown quantity, even though it had been accurately determined in [1]. The relevant robot model is given by

$$H(q)=\begin{bmatrix} a_1+2a_2c_2+(p_1+2p_2c_2)a_9 & (a_3+a_2c_2)+(p_3+p_2c_2)a_9 \\ (a_3+a_2c_2)+(p_3+p_2c_2)a_9 & a_7+p_3a_9 \end{bmatrix}$$

$$C(q,\dot{q})=s_2(a_2+p_2a_9)\begin{bmatrix} -\dot{q}_2 & -(\dot{q}_1+\dot{q}_2) \\ \dot{q}_1 & 0 \end{bmatrix}$$

$$F=\begin{bmatrix} a_4 & 0 \\ 0 & a_8 \end{bmatrix},\ g(q)=\begin{bmatrix} a_5c_1+a_6c_{12}+(p_4c_1+p_5c_{12})a_9 \\ a_6c_{12}+(p_5c_{12})a_9 \end{bmatrix}$$

where $a_1 = 6.33$, $a_2 = 0.14$, $a_3 = 0.11$, $a_4 = 27.6$, $a_5 = 31.9$, $a_6 = 3.30$, $a_7 = 0.94$, $a_8 = 4.54$, $a_9 = 1.25$ and $p_1 = 0.37$, $g_2 = 0.18$, $p_3 = 0.18$, $p_4 = 4.23$, and $p_5 = 4.15$. In the regressor formulation, the manipulator model is given by $Y_ka_k + Y_ua_u = \tau$ where

$$Y_k = \begin{bmatrix} \hat{x}_1 & 2c_2\hat{x}_1+c_2\dot{x}_2-2s_2x_1x_2-s_2x_2^2 & \dot{x}_2 & x_1 & c_2 & c_{12} & 0 & 0 \\ 0 & c_2\dot{x}_1+s_2x_1^2 & \dot{x}_1 & 0 & 0 & c_{12} & \dot{x}_2 & x_2 \end{bmatrix}$$

is the regressor associated with the known parameters $a_k = [a_1 \cdots a_8]^T, p = [p_1 \cdots p_5]^t$ and

$$Y_u = \begin{bmatrix} (p_1+2p_2c_2)\dot{x}_1+(p_3+p_2c_2)\dot{x}_2-2p_2s_2x_1x_2-p_2s_2x_2^2+p_4c_1+p_5c_{12} \\ (p_3+p_2c_2)\dot{x}_1+p_3\dot{x}_2+p_2s_2x_1^2+p_5c_{12} \end{bmatrix}$$

is the regressor associated with the unknown parameter $a_9 = m_3$. The velocities of joint angles one and two are denoted by x_1 and x_2, respectively. The implementation of the observer will be detailed presently.

B. Approximate Implementation of the Observer

The velocity estimate provided by the reduced-order adaptive velocity observer at the ith time instant was calculated with

$$\hat{x}(i)=\hat{x}(i-1)+\Delta v(i-1)+K(q(i)-q(i-1)) \\ -\Delta K\hat{x}(i-1)$$

where

$$v(i-1)=\hat{H}^{-1}(q(i-1))[\tau-\hat{C}(q(i-1), \\ \hat{x}(i-1))\hat{x}(i-1)-F\hat{x}(i-1)-\hat{g}(\hat{x}(i-1))]$$

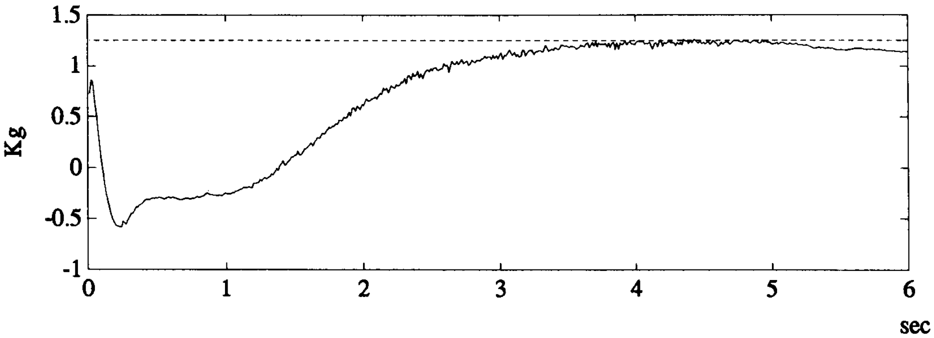

(a)

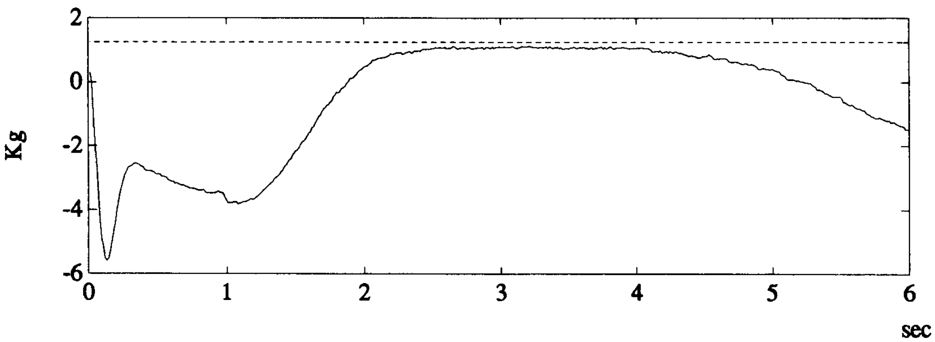

(b)

Fig. 6. Simulation: comparison of parameter adaptation (a) adaptive observer method, (b) Slotine-Li method with differentiation.

The estimates of $H(q), C(q, x)$ and $g(q)$ used in the above are given by

$$\hat{H}(q)=\begin{bmatrix} a_1+2a_2c_2+(p_1+2p_2c_2)\hat{a}_9 & (a_3+a_2c_2)+(p_3+p_2c_2)\hat{a}_9 \\ (a_3+a_2c_2)+(p_3+p_2c_2)\hat{a}_9 & a_7+p_3\hat{a}_9 \end{bmatrix}$$

$$\hat{C}(q,\hat{x})=s_2(a_2+p_2\hat{a}_9)\begin{bmatrix} -\hat{x}_2 & -(\hat{x}_1+\hat{x}_2) \\ \hat{x}_1 & 0 \end{bmatrix},$$

$$\hat{g}(q)=\begin{bmatrix} a_5c_1+a_6c_{12}+(p_4c_1+p_5c_{12})\hat{a}_9 \\ a_6c_{12}+(p_5c_{12})\hat{a}_9 \end{bmatrix}$$

These were created by replacing the third link's mass $a_9 = m_3$ with estimate $\hat{a}_9 = \hat{m}_3$. The initial estimate chosen for m_3 was $\hat{a}_9(0) = 0$. The initial velocity estimate was purposefully set at $\hat{x}(0) = [10 \quad -10]'$ degrees per second, even though the trajectory starts from rest. This was done to show the response of the observer to incorrect initial conditions.

C. Implementation of the Controller

The ith torque signal was calculated as

$$\begin{aligned}\tau(i) &= Y_{kctr}(q(i), \hat{x}(i), x_r(i), \dot{x}_d(i))a_k(i) \\ &\quad + \hat{Y}_{uctr}(q(i), \hat{x}(i), x_r, \dot{x}_d(i))\hat{a}_9(i) \\ &\quad - K_d\hat{s}(i) - K_p(q(i) - q_d(i))\end{aligned}$$

where

$$Y_{kctr} = \begin{bmatrix} \dot{x}_{d1} & 2c_2\dot{x}_{d1}+c_2\dot{x}_{d2}-s_2\hat{x}_2x_{r1}- s_2\hat{x}_1x_{r2}-s_2\hat{x}_2x_{r2} & \dot{x}_{d2} & \hat{x}_1 & c_2 & c_{12} & 0 & 0 \\ 0 & c_2\dot{x}_{d1}+s_2\hat{x}_1x_{r1} & \dot{x}_{d1} & 0 & 0 & c_{12} & \dot{x}_{d2} & \hat{x}_2 \end{bmatrix}$$

was the regressor used in control associated with the known dynamic parameters and the equation at the bottom of the page was the regressor used in control associated with the unknown dynamic parameter.

D. Parameter Adaptation

The ith parameter estimate $\hat{a}_9(i)$ was calculated with

$$\begin{aligned}\hat{a}_9(i) &= \hat{a}_9(i-1) - \gamma[\hat{Y}_{uobs}(i-1) + \hat{Y}_{uctr}(i-1)]^T \\ &\quad \cdot [q(i) - q(i-1)] - \gamma\Delta[\hat{Y}^T_{uobs}(i-1)\hat{x}(i-1) \\ &\quad + \hat{Y}^T_{uctr}(i-1)(q(i-1) - q_d(i-1) - x_d(i-1))]\end{aligned}$$

where $\Gamma = I$ was used for the adaptation gain, $\hat{Y}_{uctr}$ was defined

$$\hat{Y}_{uctr} = \begin{bmatrix} (p_1+2p_2c_2)\dot{x}_{d1} + (p_3+p_2c_2)\dot{x}_{d2} - p_2s_2\hat{x}_1x_{r2} - p_2s_2x_{r1}\hat{x}_2 - p_2s_2\hat{x}_2x_{r2} + p_4c_1 + p_5c_{12} \\ (p_3+p_2c_2)\dot{x}_{d1} + p_3\dot{x}_{d2} + p_2s_2\hat{x}_1x_{r1} + p_5c_{12} \end{bmatrix}$$

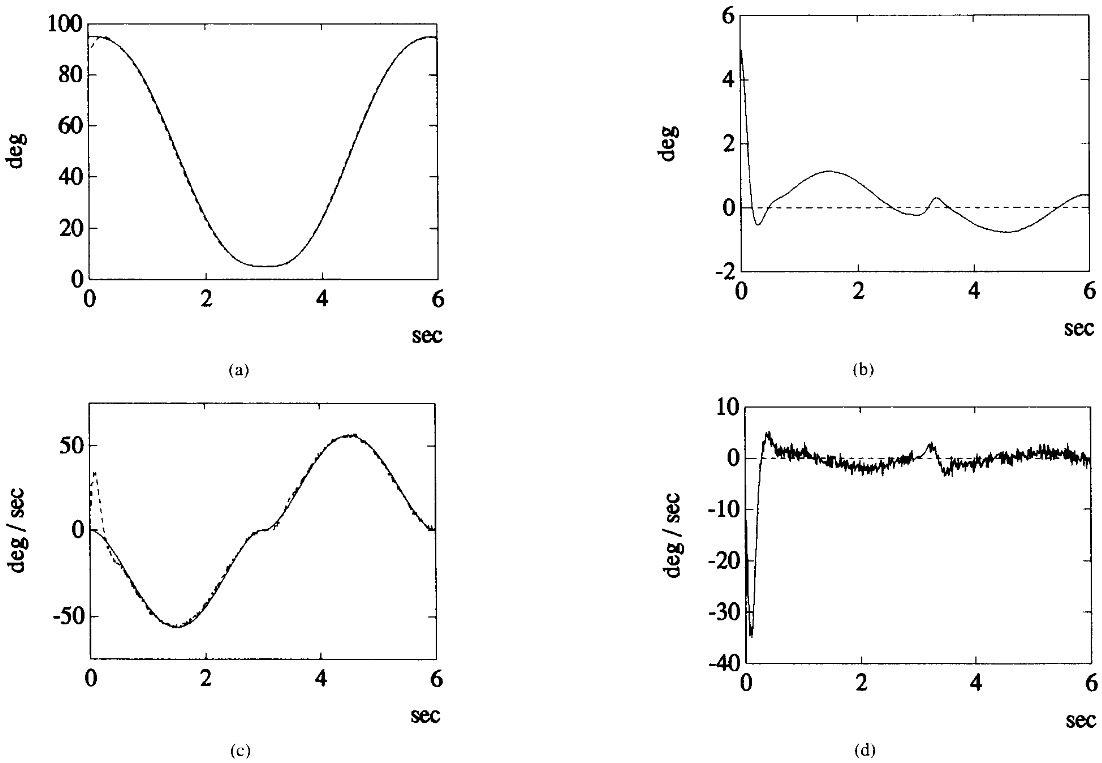

Fig. 7. Experimental results for the first link using the adaptive observer (a) desired versus measured position, (b) position error, (c) desired versus measured velocity, (d) velocity error.

as above and

$$Y_{aobs} = \begin{bmatrix} (p_1+2p_2c_2)v_1+(p_3+p_2c_2)v_2-2p_2s_2\hat{x}_1\hat{x}_2-p_2s_2\hat{x}_2^2+p_4c_1+p_5c_{12} \\ (p_3+p_2c_2)v_1+p_3v_2+p_2s_2\hat{x}_1^2+p_5c_{12} \end{bmatrix}$$

E. The Joint Trajectory and Sampling Rates

In order to test the trajectory tracking capability of the proposed adaptive observer-controller and compare results to those obtained from the well-known Slotine-Li adaptive controller, fifth order polynomial trajectories were designed for both the first and second joints of the robot manipulator (see Figs. 1(a) and 2(a)). A set of 500 points on the trajectory were provided to the controller every 12 milliseconds (msec), producing a trajectory duration of 6 seconds. The control update period was selected as $\Delta = 4$ msec.

The trajectory characteristics are as follows: the range of the trajectories for the first and second joints were (90, 120) degrees (deg), respectively, the maximum velocities were (56.3, 75.0) deg/sec and the maximum accelerations (57.7, 77.0) deg/sec^2, respectively. The trajectories described here were used for all the simulations and experiments considered in this paper.

F. Simulation Results

This section compares the proposed observer-controller with Slotine-Li's adaptive controller in which filtered position signals are differentiated to obtain velocity estimates for use in control. The comparison of the two schemes is based on computer simulation. The fifth order polynomials described above were used as the desired trajectory and the position measurement had zero-mean Gaussian noise with standard deviation $\sigma_n = 0.0818$ degrees. This noise statistic was derived from experiments conducted on a hydraulic robot arm located at International Submarine Engineering Ltd. of Port Coquitlam, British Columbia. The arm was fitted with rotary potentiometers to obtain position measurements.

The observer gains for the proposed method were chosen as $K = \mathrm{diag}(30, 20)$. To reduce the negative effect of the measurement noise on numerical differentiation in Slotine-Li's method, lowpass filters were used, i.e.

$$q_{1f}(s) = \frac{k_1}{s+k_1} q_1(s) \quad \text{and} \quad q_{2f}(s) = \frac{k_2}{s+k_2} q_2(s)$$

where s is the complex variable, $q_i(s)$ is the measured position of joint i, $q_{if}(s)$ is the filtered position of joint i and the filter gains for the first and second joint were selected as $k_1 = 30$ and $k_2 = 20$. The position and derivative gains for the proposed controller were taken as $K_p = \mathrm{diag}(500, 500)$ and $K_d = \mathrm{diag}(2\sqrt{500}, 2\sqrt{500})$, respectively. Equivalent gains were used for Slotine-Li's method.

The position and velocity tracking results for the proposed method are shown in Figs. 1 and 2. Results for Slotine-Lis method are shown in Figs. 3 and 4. Comparison of the position tracking performance for the two methods shows substantial difference, where due to the delays introduced with the position filter, control with Slotine-Li's method leads to larger errors. The maximum tracking errors for joints one and two after the first one second of motion using the proposed method were found to be 0.3 deg and 0.4 deg, respectively. Using Slotine-Li's method, these errors were found to be 1.8 deg and 3.4

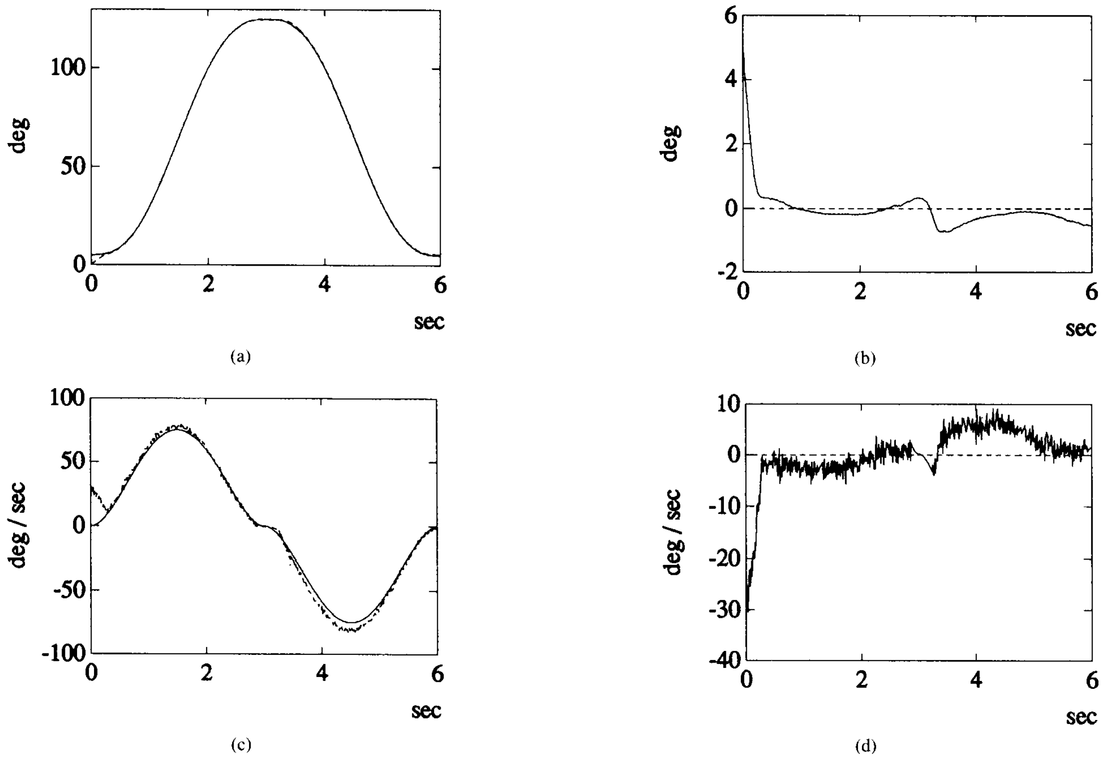

Fig. 8. Experimental results for the second link using the adaptive observer (a) desired versus measured position, (b) position error, (c) desired versus measured velocity, (d) velocity error.

deg. The velocity tracking for the two methods also differed. For the proposed method, these errors were found to be 0.63 deg/sec and 1.7 deg/sec for joints one and two after the first one second of motion and for Slotine-Li's method these were determined as 2.5 deg/sec and 5.2 deg/sec for joints one and two. It must be emphasized that the improved tracking results achieved required less torque compared to Slotine-Lis method, see Fig. 5. The 1-norm was used to quantify the average torque applied in achieving the results described above. For the proposed method, these were calculated as 27 N and 6.4 N. For Slotine-Lis method, the torques were found to be 29 N and 6.5 N.

The adaptation of the unknown parameter $\hat{a}_9(t)$ for both methods is shown in Fig. 6. The adaptive gain used in both techniques was taken as $\gamma = 5$. The dashed lines in Fig. 6(a) and (b) represent the actual value of the "unknown" parameter. The dynamics of parameter adaptation for the proposed method drifts less than that for Slotine-Li's method. Reason for this may be due to filtering which is used in Slotine-Li's method. Note that a proper regressor formulation in the adaptation rule would require the filter model in addition to the manipulator dynamics.

G. Experimental Results

Experimental testing was carried out on PUMA-560. The observer gain used was $K = \mathrm{diag}(100, 100)$, the adaptation gain was selected as $\gamma = 1.5$ and the controller gains were the same as that for the simulations above. The results of the experiment are shown in Figs. 7, 8, and 9. Figs. 7(a), 7(b) and 8(a), 8(b) show that after the initial transient, the maximum position tracking error does not exceed 1 degree for both the first and second joints over the entire six second trajectory. The velocity tracking results are shown in Figs. 7(c), 7(d) and 8(c), 8(d). The torques applied to the joints and parameter adaptation are shown in Fig. 9. Note the low level of chattering in the torque signals as well as the smooth adaptation of the unknown parameter to its actual value. The mass of the end-effector was known to be $m_3 = 1.25$ Kg from [1].

VI. Conclusion

A reduced-order adaptive velocity observer has been combined with an adaptive controller for robot manipulator trajectory control. The resulting robot-observer-controller dynamic system produces locally asymptotically stable observer velocity errors and locally asymptotically stable position and velocity tracking errors.

The adaptive observer was designed to have reduced order dynamics; that is, it exhibits a first order dynamic response as opposed to a second order response which is the case for a full order observer. In addition, high frequency switching which is a result of variable structure compensation is not required to maintain stability. The result is a smooth implementation of the observer which reduces the possibility of exciting unmodeled higher frequency dynamics of the manipulator. A by-product of the reduced chattering in the applied control torque is less mechanical wear and less energy consumption.

The observer-controller was implemented on a PUMA-560 to show that sound tracking results could be attained in practice. Simulations were also made to compare the proposed system with the well known Slotine-Li adaptive controller which used joint velocities obtained through numerical differentiation of filtered position signals. It was found that the proposed observer-controller obtained smaller position

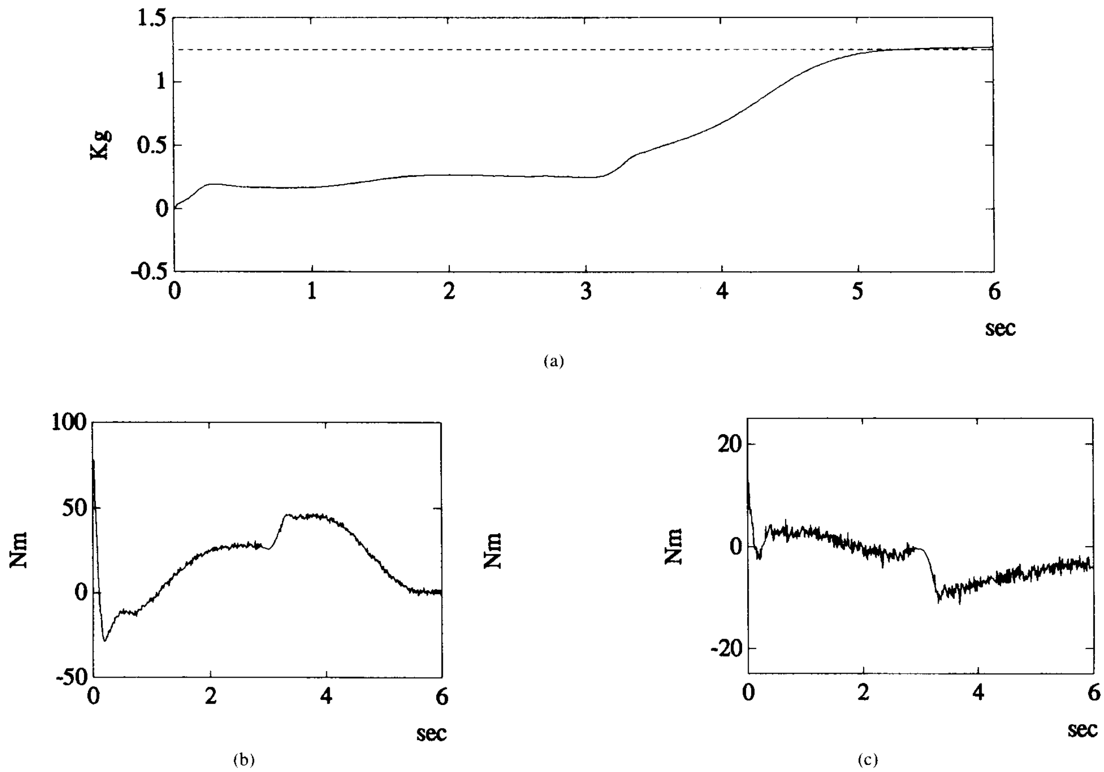

Fig. 9. Experimental results using the adaptive observer (a) parameter adaptation, (b) joint torque 1, (c) joint torque 2.

and velocity tracking errors while using less applied torque in doing so.

Appendix A

Proof of Theorem 1: Consider the Lyapunov function

$$v(t) = \tfrac{1}{2}e(t)^T P e(t)$$

where $e^T = [\tilde{x}^T \ \ \tilde{a}^T]$ and $P = \mathrm{diag}(H(q), \Gamma^{-1})$ with $\Gamma > 0$. It follows that

$$\tfrac{1}{2}p_l\|e(t)\|^2 \leq v(t) \leq \tfrac{1}{2}p_u\|e(t)\|^2. \tag{A.1}$$

The time derivative of $v(t)$ along trajectories of $\tilde{x}$ and $\tilde{a}$ is computed as

$$\dot{v} = \tilde{x}^T\left(H(q)\dot{\tilde{x}} + \tfrac{1}{2}\dot{H}(q)\tilde{x}\right) + \tilde{a}^T\Gamma^{-1}\dot{\tilde{a}}. \tag{A.2}$$

Subtracting (5) from (4), we have

$$H(q)\dot{\tilde{x}} = -C(q,\hat{x})\tilde{x} - C(q,x)\tilde{x} - F\tilde{x} - H(q)K\tilde{x} + \Theta \tag{A.3}$$

where

$$\Theta = \tilde{H}(q)w + \tilde{C}(q,\hat{x})\hat{x} + \tilde{F}\hat{x} + \tilde{g}(q)$$

By applying property 5, (A.3) becomes

$$\begin{aligned}H(q)\dot{\tilde{x}} = &-C(q,\hat{x})\tilde{x} - C(q,x)\tilde{x} - F\tilde{x}\\ &-H(q)K\tilde{x} + Y(q,\hat{x},w)\tilde{a}\end{aligned} \tag{A.4}$$

where $\tilde{H} = \hat{H} - H, \tilde{C} = \hat{C} - C, \tilde{F} = \hat{F} - F$, and $\tilde{g} = \hat{g} - g$. Now, substituting (A.4) into (A.2) and using properties 3 and 4, we have

$$\begin{aligned}\dot{v} = &-\tilde{x}^T(H(q)K + F + C(q,\hat{x}))\tilde{x}\\ &+ \tilde{a}^T[\Gamma^{-1}\dot{\tilde{a}} + Y^T(q,\hat{x},w)\tilde{x}]\end{aligned} \tag{A.5}$$

which in conjunction with (6) and properties 1 and 2 gives

$$\dot{v}(t) \leq -(\underline{\sigma} + m_f - m_c m_v - m_c\|\tilde{x}\|)\|\tilde{x}\|^2 \tag{A.6}$$

Hence $\dot{v}(t) \leq -\beta\|\tilde{x}(t)\|^2$ if

$$\underline{\sigma} > m_c\|\tilde{x}\| + m_c m_v + \beta - m_f \tag{A.7}$$

where $\beta > 0$ is a fixed constant. Since $\|e\| > \|\tilde{x}\|$, (A.7) holds if

$$\|e\| < \frac{1}{m_c}(\underline{\sigma} + m_f - \beta) - m_v \tag{A.8}$$

From (A.6), (A.8) and (A.1), it follows that if

$$\|e(0)\| < \sqrt{\frac{p_l}{p_u}}\left[\frac{1}{m_c}(\underline{\sigma} + m_f - \beta) - m_v\right] \tag{A.9}$$

then

$$\dot{v}(t) \leq -\beta\|\tilde{x}(t)\|^2 \qquad \forall t \geq 0 \tag{A.10}$$

By (A.1) and (A.10), $\tilde{x}(t) \in L_\infty$ and $\tilde{x}(t) \in L_2$. Furthermore, (A.1) and $\dot{v}(tO < 0$ implies that $\tilde{a}(t) \in L_\infty$, thus $\hat{a}(t) = \tilde{a} + a \in L_\infty$. So $w(q, \hat{x}, \tau, \hat{a})$ as a time function belongs to L_∞ if is bounded. Now by (A.4) it can be seen that $\dot{\tilde{x}}(t) \in L_\infty$. Thus Barbalat's lemma [9, p. 25] implies that $\tilde{x}(t) \to 0$ as $t \to \infty$.

Appendix B

Proof of Theorem 2: Define

$$v(t) = \tfrac{1}{2}e(t)^T P e(t)$$

where $e^T = [s^T \ \ \tilde{x}^T \ \ \tilde{q}^T \ \ \tilde{a}^T]$ and $P = \mathrm{diag}(H(q), H(q), K_p, \Gamma^{-1})$ with $K_p = K_p^T > 0$ and $\Gamma > 0$. Then $v(t)$ satisfies

$$\tfrac{1}{2}p_l\|e(t)\|^2 \leq v(t) \leq \tfrac{1}{2}p_u\|e(t)\|^2 \tag{B.1}$$

The time derivative $v(t)$ of along trajectories of $e(t)$ is given by

$$\dot{v} = s^T\left(H(q)\dot{s} + \frac{\dot{H}(q)}{2}s\right) + \dot{\tilde{q}}^T K_p\tilde{q} + \tilde{x}^T\left(H(q)\dot{\tilde{x}} + \frac{\dot{H}(q)}{2}\right) + \tilde{a}^T\Gamma^{-1}\dot{\tilde{a}} \tag{B.2}$$

As $\dot{\tilde{a}} = \dot{\hat{a}}$ and $\dot{\tilde{q}} = s - \tilde{q}$, (B.2) becomes

$$\dot{v} = s^T\left(H(q)\dot{s} + K_p\tilde{q} + \frac{\dot{H}(q)}{2}s\right) - \tilde{q}^T K_p\tilde{q} + \tilde{x}^T\left(H(q)\dot{\tilde{x}} + \frac{\dot{H}(q)}{2}\tilde{x}\right) + \tilde{a}^T\Gamma^{-1}\dot{\hat{a}} \tag{B.3}$$

The controller's error dynamics is found by equating (1) and (15) and applying properties 3, 4, and 5 along with the fact that

$$\begin{aligned} &H(q)\dot{x} - \hat{H}(q)[\dot{x}_r + \dot{\tilde{x}}] \\ &= H(q)\dot{s} - \tilde{H}(q)(\dot{x}_d - (\dot{\hat{x}} - \dot{x}_d)) - H(q)\dot{\tilde{x}} \end{aligned}$$

to obtain

$$\begin{aligned} H(q)\dot{s} = &- C(q,x)s - (K_d + F)s - K_p\tilde{q} + K_d\tilde{x} \\ &+ H(q)\dot{\tilde{x}} - C(q,x_r)\tilde{x} + Y(q,\hat{x},x_r,\dot{x}_d)\tilde{a} \end{aligned} \tag{B.4}$$

where $s = x - x_r = \dot{\tilde{q}}_{\tilde{q}}$. The observer error dynamics was given by (A.4). Substituting (B.4), (A.4), and (16) into (B.3) and using property 4 gives

$$\begin{aligned} \dot{v} = &- s^T(K_d + F)s - \tilde{q}^T K_p\tilde{q} - \tilde{x}^T(H(q)K \\ &+ F + C(q,\dot{x}))\tilde{x} + s^T(K_d + H(q) \\ &- C(q,x_r))\tilde{x}. \end{aligned} \tag{B.5}$$

As $x_r = x_d - \tilde{q}$ and $\hat{x} = x_d + s - \tilde{x} - \tilde{q}$, (B.5) implies that

$$\begin{aligned} \dot{v} \le &- (k_d + m_f)\|s\|^2 - (\underline{\sigma} + m_f - m_c m_d \\ &- m_c(\|\tilde{x}\| + \|s\| + \|\tilde{q}\|))\|\tilde{x}\|^2 - k_p\|\tilde{q}\|^2 \\ &+ (k_d + m_u + m_c(m_d + \|\tilde{q}\|))\|\tilde{x}\|\|s\|] \end{aligned} \tag{B.6}$$

where $\|x_d\| \le m_d$, $K_d = k_d I$, $k_p = \lambda_{\min}(K_p)$ and $m_f = \lambda_{\min}(F)$ have been used. Writing (B.6) as

$$\dot{v} = -[\|s\| \quad \|\tilde{x}\| \quad \|\tilde{q}\|]B(\|s\|,\|\tilde{x}\|,\|\tilde{q}\|)[\|s\| \quad \|\tilde{x}\| \quad \|\tilde{q}\|]^T \tag{B.7}$$

it can be verified readily that B is positive definite if

$$\underline{\sigma} > c - \frac{b^2}{4a} - m_f + \beta \tag{B.8}$$

and

$$\|e(t)\| < \frac{\sqrt{4a(\underline{\sigma} + m_f - \beta) - 4ac} - b}{2a} \tag{B.9}$$

where a, b and c are given by (19). Note that (B.7), (B.8) and (B.9) imply that

$$\dot{v}(t) \le -\beta\left\|\begin{bmatrix} s \\ \tilde{x} \\ \tilde{q}\end{bmatrix}\right\|^2 \tag{B.10}$$

where β is the infimum of the smallest eigenvalue of B. It now follows from (B.1) that (B.10) remains valid for $t \ge 0$, if the initial error vector $e(0)$ satisfies

$$\|e(0)\| < \sqrt{\frac{p_l}{p_u}}\left[\frac{\sqrt{4a(\underline{\sigma} + m_f - \beta) + b^2 - 4ac} - b}{2a}\right].$$

Note from (B.1) and (B.10) that $s, \tilde{x}, \tilde{q}, \tilde{a} \in L_p\infty$. In addition, from (B.10) we conclude $s, \tilde{x}, \tilde{q} \in L_2$. To show $\dot{s}, \dot{\tilde{x}} \in L_\infty$, express (B.4) and (A.4) explicitly for $\dot{s}$ and $\dot{\tilde{x}}$. For $\dot{s}(t)$ we have

$$\begin{aligned} \dot{s} = H^{-1}(q)[&-C(q,x)s - (K_d + F)s - K_p\tilde{q} + K_d\tilde{x} \\ &+ H(q)\dot{\tilde{x}} - C(q,x_r)\tilde{x} + Y(q,\hat{x},x_r,\dot{x}_d)\tilde{a}] \end{aligned}$$

in which $x = x_d + s - \tilde{q} \in L_\infty, x_r = x_d - \tilde{q} \in L_\infty$ and $\hat{x} = x_d + s - \tilde{x} - \tilde{q} \in L_\infty$. Hence $\dot{s} \in L_\infty$. For $\dot{\tilde{x}}$ we have

$$\begin{aligned} \dot{\tilde{x}} = &H^{-1}(q)[-C(q,\hat{x})\tilde{x} - C(q,x)\tilde{x} - F\tilde{x} - H(q)K\tilde{x}] \\ &+ H^{-1}(q)[\tilde{H}(q)v + \tilde{C}(q,\hat{x})\hat{x} + \tilde{F}\hat{x} + \tilde{g}(q)] \end{aligned}$$

where $x, \hat{x} \in L_\infty$ so we need only to show $v \in L_\infty$. Furthermore, since

$$v(q,\hat{x},\tau,\hat{a}) = \hat{H}^{-1}(q)[\tau - \hat{c}(q,\hat{x})\hat{x} - \hat{F}\hat{x} - \hat{g}(q)]$$

we need only show to $\tau \in L_\infty$. To do this we recognize that all signals in controller (6) belong to L_∞. Therefore $\dot{s}, \dot{\tilde{x}} \in L_\infty$.

For the observer we have $\tilde{x}, \dot{\tilde{x}} \in L_\infty$ and $\tilde{x} \in L_2$. Proceeding with Barbalat's lemma we conclude $\tilde{x}(t) \to 0$ as $t \to \infty$. Similarly, for the controller we have $s, \dot{s} \in L_\infty$ and $s \in L_2$ which implies $s(t) \to 0$ as $t \to \infty$. Finally, since $s = \dot{\tilde{q}} + \tilde{q}$ is a stable filter $s(t) \to 0$ implies that both $\tilde{q}(t) \to 0$ and $\dot{\tilde{q}}(t) \to 0$ as $t \to \infty$.

REFERENCES

[1] B. Armstrong, O. Khatib, and J. Burdick, "The explicit dynamic and inertial parameters of the PUMA 560 arm," in *Proc. IEEE Int. Conf. Robot. and Automat.*, 1986, pp. 510–518.

[2] A. K. Bejczy, "Robot arm dynamics and control," Jet Propulsion Laboratory, California Institute of Technology, 1974.

[3] J. J. Craig, P. Hsu, and S. S. Sastry, "Adaptive control of mechanical manipulators," in *Proc. IEEE Int. Conf. Robot. and Automat.*, 1986, pp. 190–95.

[4] M. Erlic and W.-S. Lu, "Computer independent driver-sensor interface for closed loop control of a mechanical manipulator," in *Proc. Canadian Conf. Elect. and Comput. Eng.*, 1989, pp. 504–507.

[5] M. Erlic and W.-S. Lu, "Manipulator control with and exponentially stable velocity observer," in *Proc. Amer. Cont. Conf.*, 1991, pp. 1241–42.

[6] R. Johansson, "Adaptive control of robot manipulator motion," *IEEE Trans. Robot. and Automat.*, vol. 6, pp. 483–90, 1990.

[7] D. G. Luenberger, "Observing the state of linear systems," *IEEE Trans. Military Electron.*, vol. 8, pp. 74–90, 1964.

[8] S. Nicosia and P. Tomei, "Robot control by using only position measurements," *IEEE Trans. Automat. Cont.*, vol. 35, pp. 1058–1061, 1990.

[9] S. Sastry and M. Bodson, *Adaptive Control, Stability, Convergence, and Robustness.* Englewood Cliffs, N.J: Prentice Hall, 1989.

[10] J.-J. E. Slotine and W. Li, "Adaptive manipulator control: A case study," *IEEE Trans. Automat. Cont.*, vol. 33, pp. 995–1003, 1988.

[11] M. W. Spong and M. Vidyasagar, *Robot Dynamics and Control.* New York, NY: Wiley, 1989.

[12] C. Canudas de Wit, K. J. Astrom, and N. Fixot, "Computed torque control via a nonlinear observer," *Int. J. Adaptive Cont. and Signal Processing*, vol. 4, pp. 443–452, 1990.

[13] C. Canudas de Wit and N. Fixot, "Adaptive control of robot manipulators via velocity estimated feedback," in *Proc. IEEE Int. Conf. Robot. and Automat.*, 1991, pp. 16–21.